9-1-2016

Chemical modification of extracellular matrix by cold atmospheric plasma-generated reactive species affects chondrogenesis and bone formation.

Peter Eisenhauer
Thomas Jefferson University

Natalie Chernets
Thomas Jefferson University

You Song
Thomas Jefferson University

Danil Dobrynin
Drexel University

Nancy Pleshko
Temple University

See next page for additional authors

HHS Public Access

Author manuscript

J Tissue Eng Regen Med. Author manuscript; available in PMC 2017 November 13.

Published in final edited form as:

J Tissue Eng Regen Med. 2016 September ; 10(9): 772–782. doi:10.1002/term.2224.

Chemical modification of extracellular matrix by cold atmospheric plasma-generated reactive species affects chondrogenesis and bone formation

Peter Eisenhauer[1], **Natalie Chernets**[1], **You Song**[1], **Danil Dobrynin**[2], **Nancy Pleshko**[3], **Marla J. Steinbeck**[4], and **Theresa A. Freeman**[1,2,*]

[1]Department of Orthopaedic Surgery, Thomas Jefferson University, Philadelphia, PA, USA

[2]Drexel Plasma Institute, Drexel University, Philadelphia, PA, USA

[3]Department of Bioengineering, Temple University, Philadelphia, PA, USA

[4]School of Biomedical Engineering, Science and Health Systems, Drexel University, Philadelphia, PA, USA

Abstract

The goal of this study was to investigate whether cold plasma generated by dielectric barrier discharge (DBD) modifies extracellular matrices (ECM) to influence chondrogenesis and endochondral ossification. Replacement of cartilage by bone during endochondral ossification is essential in fetal skeletal development, bone growth and fracture healing. Regulation of this process by the ECM occurs through matrix remodelling, involving a variety of cell attachment molecules and growth factors, which influence cell morphology and protein expression. The commercially available ECM, Matrigel, was treated with microsecond or nanosecond pulsed (μsp or nsp, respectively) DBD frequencies conditions at the equivalent frequencies (1 kHz) or power (~1 W). Recombinant human bone morphogenetic protein-2 was added and the mixture subcutaneously injected into mice to simulate ectopic endochondral ossification. Two weeks later, the masses were extracted and analysed by microcomputed tomography. A significant increase in bone formation was observed in Matrigel treated with μsp DBD compared with control, while a significant decrease in bone formation was observed for both nsp treatments. Histological and immunohistochemical analysis showed Matrigel treated with μsp plasma increased the number of invading cells, the amount of vascular endothelial growth factor and chondrogenesis while the opposite was true for Matrigel treated with nsp plasma. In support of the *in vivo* Matrigel study, 10 T1/2 cells cultured *in vitro* on μsp DBD-treated type I collagen showed increased expression of adhesion proteins and activation of survival pathways, which decreased with nsp plasma treatments. These results indicate DBD modification of ECM can influence cellular behaviours to accelerate or inhibit chondrogenesis and endochondral ossification.

*Correspondence to: T. Freeman, Department of Orthopaedic Surgery, Thomas Jefferson University, Curtis Building, Room 501, 1015 Walnut Street, Philadelphia, PA 19107-5099, USA. theresa.freeman@jefferson.edu.

Conflict of interest

The authors have declared that there is no conflict of interest.

Supporting information

Additional supporting information may be found in the online version of this article at the publisher's web-site.

Keywords

bone; FTIR; plasma; matrigel; chondrogenesis; endochondral ossification

1. Introduction

Plasma medicine is the clinical application of cold (non-thermal or non-equilibrium) plasma to directly treat cells and tissues. Clinical applications of cold plasma currently in development include the sterilization of wounds and burns, improved wound healing and eradication of cancer cells (Fridman *et al.*, 2006; Brulle *et al.*, 2012; Chernets *et al.*, 2015; Daeschlein *et al.*, 2015; Li *et al.*, 2015; Siu *et al.*, 2015; Ulrich *et al.*, 2015). The successful use of cold plasma for these applications has led to questions concerning the mechanisms of how these treatments affect cell and tissue function. The authors' laboratory has shown that a short cold plasma treatment (10 s) of mesenchymal cells with microsecond pulsed (μsp) dielectric barrier discharge (DBD) increases intracellular reactive oxygen species (ROS) and ROS-associated signalling to enhance both chondrogenic and osteogenic differentiation (Steinbeck *et al.*, 2013). It has also been shown that a single (10 s) plasma treatment of murine limb autopods in culture accelerates their development, survival and growth/elongation (Chernets *et al.*, 2014) by activating ROS-associated signalling pathways. In addition, nanosecond pulsed (nsp) DBD for longer periods of time (minutes) effectively killed cancer cells and eradicated melanoma tumours through the chemical reactions of ROS and reactive nitrogen species (RNS) generated within the tissue (Chernets *et al.*, 2015).

While plasma-generated ROS and RNS are critical components responsible for the effectiveness of plasma in wound healing, cancer treatment and bactericidal applications, other biophysical stimuli present within the plasma include local and global electric fields, shock waves and radiation (Fridman, 2008; Fridman *et al.*, 2008; Kong *et al.*, 2009). The amount of each of these biophysical stimuli is largely dependent upon the type of plasma and the treatment parameters (Liu *et al.*, 2014). Cold plasma characteristics can be tuned for each specific biological application by adjusting the timing, voltage, power, frequency and type of electrode. In addition, plasma-generating devices (pulsers) capable of creating faster pulse rates (microsecond, nanosecond and picosecond ranges) have been developed. Compared with μsp DBD, nsp DBD produces an increased pulse rate with an applied voltage approximately 1000 times faster (7.8 kV/ns), creating a more uniform discharge. A uniform discharge is thought to decrease the damage to cells and tissues as fewer current channels, streamers or filaments (multigenerational accumulation of streamers, like small lightning bolts) are formed within the plasma. However, the plasma produced at the higher pulse rate also generates greater/cytotoxic concentrations of ROS and RNS (Liu *et al.*, 2014; Zhang *et al.*, 2014). To date, there has been a lack of studies characterizing each plasma type and condition, which has led to a disconnect in determining how the different plasmas affect biological tissues and cellular processes (Jiang *et al.*, 2009; Duval *et al.*, 2013; Alekseev *et al.*, 2014; Li *et al.*, 2014). To further confound our understanding, isolated cells treated with plasma also tend to react much differently than treated tissues (unpublished data). This is most probably because of the differential effects of plasma-generated ROS, RNS and

biophysical forces on each cell type within a tissue, the extracellular matrix (ECM) molecules interspersed between cells or a combination of effects on cells and ECM.

As a first step in determining the biological difference between μsp and nsp DBD plasmas, the commercially available ECM, Matrigel (BD Bioscience, Inc., Franklin Lakes, NJ, USA), was treated with each type of DBD as part of a murine ectopic ossification model. In this model, it was shown that μsp DBD treatment enhanced cell numbers, cartilage differentiation and increased bone formation of the Matrigel ectopic masses. Conversely, treatment of the Matrigel with nsp DBD, using the same frequency or power as the μsp DBD, had the opposite effect and significantly decreased cell number, slowed cartilage differentiation and reduced bone formation. The present study highlights the ability of DBD treatments to directly modify ECM and indirectly affect cell behaviour and tissue function. In this way, DBD treatment of ECM can be tuned to either negatively or positively influence cell–matrix interactions in tissue engineering or clinical applications. Furthermore, understanding the effects of plasma on ECM, and not only on cells, is critical for developing plasma as a tool for use in any biomedical application.

2. Materials and methods

2.1. Animals

For the experiment, C57BL/6 mice aged 8–12 weeks were obtained from Charles River laboratory (Wilmington, MA, USA). The abdominal region was visually divided into four quadrants and 250 μl Matrigel was injected subdermally into each quadrant (see section 2.3). All animals were euthanized at the 2-week time-point according to National Institutes of Health (NIH) guidelines for the care and use of laboratory animals and all animal protocols were approved by the Institutional Animal Care and Use Committee (IACUC) at Thomas Jefferson University, Philadelphia, PA, USA.

2.2. Cold plasma treatment of Matrigel

Growth Factor Reduced, Phenol Red Free, Corning Matrigel Basement Membrane Matrix (BD Bioscience, Inc.) were thawed from −20°C to 4°C and held at 4°C as a liquid. Following thawing, 1 ml of liquid Matrigel was dispensed into a six-well plate for treatment using a 32 mm plasma electrode (Steinbeck *et al.*, 2013). Plasma treatment of Matrigel was performed at 4°C with DBD similar to the procedure described by Fridman *et al.* (2006), where the schematics, voltage and current curves of the power supply (Plasma Power, LLC, Philadelphia USA) are detailed. The μsp DBD treatment voltage, frequency, pulse width and probe were based on previous publications (Steinbeck *et al.*, 2013; Chernets *et al.*, 2015). Briefly, μsp DBD treatment was generated at the voltage of 20 kV (peak to peak), a typical rise time of 5 V/ns and a pulse repetition rate of 1 kHz applied through a high-voltage electrode covered by 1 mm thick quartz for 1 min. In addition, a nsp-DBD treatment at a voltage of 24 kV (peak to peak), with a typical rise time of 7.8 kV/ns and a pulse repetition rate of 1 kHz or 0.1 kHz applied through a high-voltage electrode for 1 m. The plastic six-well plate was placed on a grounded metal plate and the electrode was positioned 2 mm above the liquid Matrigel. A comparison of the plasma power measurements for the 1 kHz μsp-DBD treatment (1.1 W), 0.1 kHz nsp-DBD treatment (0.8 W) and 1 kHz nsp DBD (9.7

W) are shown in Figure 1a and an image of the DBD-treatment setup is shown in Figure 1b. Following treatment, Matrigel was promptly removed from the well plate and stored on ice before injection into the mice. A small sample of Matrigel was taken for Fourier transform infrared spectroscopy (FTIR) analysis and sodium dodecyl sulphate–polyacrylamide gel electrophoresis (SDS-PAGE). This treatment protocol was repeated for each of the three treatments.

2.3. Mouse ectopic endochondral ossification assay

An experimental model of endochondral ossification was utilized by induction of ectopic bone formation, as previously described (Eaton *et al.*, 2014). Briefly, plasma-treated or untreated mixtures of Matrigel on ice (BD Bioscience, Inc.) were mixed with 3.5 μg/ml of recombinant human bone morphogenetic protein-2 (rhBMP-2; Gene Script Corp., Piscataway, NJ, USA) and after mixing aliquots (300 μl) were injected in four subcutaneous abdominal sites in 2-month-old CD-1 or C57BL/6 mice following IACUC-approved protocols. An untreated BMP-2 positive control, which represented the control (100%) response within each mouse, was always included. After 2 weeks the masses were removed and microcomputed 1tomography (μCT) analysis was performed using an X-ray tube energy of 45 kVp, a current of 177 μA and a 200-ms integration time, producing a spatial resolution of 12 μm^3 voxel size to measure bone volume over total volume (BV/TV). Each ectopic mass was then compared with the positive BMP-2 control and the per cent difference was determined. Each treatment was tested independently in at least four individual mice ($n = 8$ for 1 kHz microsecond and nanosecond, $n = 4$ for 0.1 kHz nanosecond). Values collected for BV/TV are represented as percentages of control for both variation in the size of the Matrigel mass and variation between individual mice.

2.4. Histology and Immunohistochemistry

For histological analyses, Matrigel masses from at least four different mice were collected, embedded in paraffin and sectioned at 6 μm thick for each condition (control, μsp DBD, and both nsp DBD treatments). Multiple sections from different regions were obtained from each Matrigel sample collected. The slides were deparaffinized, rehydrated and stained with Alcian Blue (cartilage), trichrome (collagen), Alizarin Red (mineralization) or Vectashield Hard Set with 4′,6-diamidino-2-phenylindole (DAPI) (count cells).

Immunohistochemistry detection with 3,3′-diaminobenzidine (DAB) was used to analyse vascular endothelial growth factor (VEGF) expression. Tissue slides were deparaffinized, rehydrated then subjected to antigen unmasking solution (Vector Labs, Burlingame, CA, USA) for 2 × 10 min at 100°C. After washing in phosphate-buffered saline (PBS), all slides were incubated with 0.5% Triton in PBS for 10 min at room temperature for permeabilization and incubated with a 3% hydrogen peroxide (H_2O_2) solution in methanol for 5 min at room temperature to block endogenous peroxidases. Blocking was performed in 4% bovine serum albumin (BSA; Equitech-Bio, Kerrville, TX, USA) with 0.1% Tween 20 in PBS for 1 h before the primary rabbit anti-VEGF (1:50; Santa Cruz Biotechnology, Inc., Dallas, TX, USA) was applied and incubated overnight at 4°C. The secondary horseradish peroxidase (HRP)-conjugated rabbit antibody (1:200; Santa Cruz Biotechnology) was applied for 1 h at room temperature, before detection with the DAB Peroxidase (HRP)

Substrate Kit (Vector Labs). A negative control sample was incubated with no primary antibody.

2.5. Fourier transform infrared imaging spectroscopy (FT-IRIS) data acquisition and analysis

To assess molecular changes associated with plasma treatment FT-IRIS images were obtained from drops of Matrigel deposited on low-e reflective-coated infrared microscope slides (MirrIR slides; Kevley Technologies, Chesterland, OH, USA). Matrigel was treated with different plasma frequencies before depositing onto low-e reflective-coated infrared microscope slides. Data were acquired in the mid-infrared region, 750–2000/cm, at 8/cm spectral resolution and 25 μm spatial resolution, with two co-added scans per pixel (15 co-added scans per pixel for background spectrum) using a Perkin Elmer Spotlight 400 Imaging Spectrometer (Shelton, CT, USA). Data were acquired from regions approximately 800 × 800 μm^2 in size, which resulted in approximately 1080 spectra per treatment. Spectral data were analysed with ISys 5.0 software (Malvern Instruments, Columbia, MD, USA). Absorbances were investigated in the spectral regions where molecular changes are reflected in protein structure, primarily the Amide I and Amide II regions, centred at ~1650/cm and 1550/cm (Barth, 2007). Second derivatives of the spectra were investigated to improve the resolution of spectra and identify absorbances that underlie the broad amide bands. The intensity of the derivative bands were multiplied by negative one to obtain positive peak heights. The FT-IRIS data were also obtained from pure type IV collagen (BD Biosciences–Discovery Labware, Bedford, MA, USA), the primary protein component of Matrigel, for comparison.

2.6. Plasma power measurements for DBD

Discharge energy was measured using P6015A high-voltage probe (75 MHz bandwidth; Tektronix, Center Valley, PA, USA) and CM-10-L current monitor (10 ns usable rise time) Ion Physics Corporation, Fremont, NH, USA) connected to a 1 GHz DPO-4104B oscilloscope (Tektronix, Center Valley, PA, USA). Before taking measurements, signals from both probes were synchronized using Tektronix AFG-3252 Arbitrary/Function Generator. Energy measurements were performed for the whole duration of voltage waveform [~200 ns for nanosecond pulser because of reflections in relatively short (~2 m) cable, and ~30 μs for microsecond pulser]. Discharge power was calculated from the energy measurements by multiplying the pulse energy by the pulse frequency.

2.7. Hydrogen peroxide, nitric oxide and peroxynitrite production by DBD plasma

Detection of reactive species in gelatin samples was performed similarly as described elsewhere (Dobrynin *et al.*, 2012; Park *et al.*, 2013). Hydrogen peroxide was detected by measuring fluorescence of 100 μM solution of Amplex UltraRed reagent in PBS (Molecular Probes, Eugene, OR, USA) at an excitation frequency of 530 nm and emission at 590 nm, with 100 U/μl of H_2O_2 (MP Biomedicals, Santa Ana, CA, USA) in 10% gelatin prepared in PBS. A 100-μl aliquot of reagent solution was added to warm liquid gelatin (1 ml), poured into six-well plates and incubated in the dark for 10 min at room temperature until solidification. Samples were then treated with DBD at fixed 2 mm distance and fluorescence was measured 5 min afterwards using an LS55 (Perkin Elmer) fluorescent spectrometer.

Nitric oxide was detected using a similar procedure. For that, 100 μl diaminofluorescein-2 (DAF-2) reagent (50 μM in dimethylsulphoxide (DMSO) excitation frequency 485 nm, emission frequency 538 nm; Cayman Chemical), was added to gelatin before solidification. Dichlorodihydrofluorescein diacetate (H_2DCFDA, 50 μl in DMSO excitation frequency 495 nm, emission frequency 518 nm; Molecular Probes) was used to detect peroxynitrite anion ($ONOO^-$) in gelatin. In addition, DMSO and horseradish peroxidase (100 U) were used as hydroxyl radical (OH) and H_2O_2 scavengers.

2.8. Collagen treatment and cell culture

A mixture of type I collagen from rat tail (#354236; BD Biosciences, Bedford, MA, USA) was prepared at a concentration 0.15 mg/ml in 0.02 N acetic acid. Collagen mixture (1 ml) was treated with DBD by the same procedure for Matrigel treatment, as described above. Following treatment, 5ml of treated collagen mixture was coated onto culture flasks and incubated for 5 min before it was removed from the flasks. The flasks were washed with PBS and allowed to air dry before cell culture. CH3/10 T1/2 cells were cultured in collagen coated flasks in Dulbecco's Modified Eagle's Medium (DMEM; Thermo Fisher, Waltham, MA, USA) containing 100 units/ml penicillin, 100 μg/ml streptomycin (Cellgro, Manassas, VA, USA), 5% fetal bovine serum (FBS; CellGro) and 5% fetal calf serum (FCS; Gemini, West Sacramento, CA, USA) to enhance cell proliferation in a 5%CO_2 incubator at 37°C. Each flask was coated with collagen treated with a specific DBD application. Cells were also cultured in an untreated collagen-coated flask and in an uncoated flask as controls. Western analysis was performed after 24 h in culture.

In addition, to visualize the actin cytoskeleton of the cells, the cells were cultured on collagen-coated glass cover slips. The collagen was either treated with one of the plasma conditions or untreated for control. The coating procedure was similar to the flask coating procedure with an incubation time of 5 min with collagen. Alexa Fluor 488® phalloidin (#A12379; Life Technologies, Carlsbad, CA, USA) was added to cell culture to visualize actin cytoskeleton at 5 μl of 6.6 μM stock/200 μl PBS (as per manufacturer instructions), and counterstained with Vectashield Hard Set with DAPI (Vector Labs).

2.9. Western analysis

Cells were lysed in Mammalian Protein Extraction Reagent (MPER; Thermo Fisher), and protein concentrations were measured using Bio-Rad Protein Assay (Bio-Rad Laboratories, Hercules, CA, USA). Approximately 40 μg of protein was loaded onto each lane of a sodium SDS-polyacrylamide gel and, after electrophoresis, the proteins were transferred to a polyvinylidene difluoride (PVDF) membrane. The membrane was blocked by incubation in Tris-buffered saline (TBS) with 0.05% Tween-20 (Thermo Fisher) and 5% Membrane Blocking Agent (GE Healthcare, Amersham, UK) for 1 h while shaking. The membranes were then incubated with their respective primary antibodies in TBS with 0.05% Tween-20 overnight at 4°C. Antibodies used for western blot included rabbit anti-pFAK (#16563), mouse anti-FAK (#1688), mouse anti-BCL-2 (#783) and goat anti-β-actin (#81178) (all from Santa Cruz Biotechnology) and rabbit anti-AKT (#92725; Cell Signaling Technology, Beverly, MA, USA). The primary antibody was removed and the blots were washed three times in TBS with 0.05% Tween-20. Their respective horseradish HRP-conjugated

secondary antibodies (Santa Cruz) were then applied to the blots which were incubated for 1 h at room temperature, washed intensively in TBS with 0.05% Tween-20 and then reacted with ECL Advanced Detection system (GE Healthcare, Amersham, UK) for 5 min at 25°C. Detection of the membranes was done with a FujiFilm Intelligent Darkbox (FujiFilm, Tokyo, Japan).

2.10. Imaging and data analysis

Images were acquired with a 12-bit cooled digital camera (Retiga Exi; QImaging, Burnaby, BC, Canada) as monochrome with optional LCD colour filter on an Eclipse E800 microscope (Nikon, Melville, NY, USA). Histomorphometric analyses were performed using Image Pro Plus 7.0 (Media Cybernetics, Silver Spring, MD, USA) to measure a ratio of area positively stained to total area. Background intensity was subtracted from each image before combining and pseudo-colouring. When the images were enhanced to clearly show localization of the protein, all images were enhanced equally. Intensity and localization analysis was performed with a custom written module to automate and standardise the procedure.

2.11. Statistical analysis

The Kruskal–Wallis test (XLstat; Addinsoft, New York, NY, USA) for one-way analysis of variance (ANOVA) in non-parametric samples was used to determine whether there were significant differences between the four groups, followed by the student's *t*-test (two-tailed distribution, two-sample unequal variance) to determine significance ($P < 0.05$). Statistical significance is indicated as * ($P < 0.05$), ** ($P < 0.01$), *** ($P < 0.001$), δ ($P < 0.05$ for μsp DBD vs. nsp DBD 0.1 kHz) and # ($P < 0.05$ for nsp DBD at 0.1 kHz compared with 1 kHz), unless specified otherwise. The data are presented as mean ± SEM.

3. Results

3.1. Treatment of the Matrigel with DBD alters bone formation in the ectopic masses

Microcomputed tomography reconstruction (Figure 1c) and Alizarin Red histological staining (Figure 1d) indicate an increased bone and mineral deposition in the μsp DBD-treated Matrigel masses, whereas a decrease was observed in the nsp DBD-treated masses, compared with control. Quantitative μCT analysis of the Matrigel masses confirmed that μsp DBD treatment significantly increased bone formation (43% increase in BV/TV; $P < 0.05$) while both nsp DBD treatments significantly decreased bone formation compared with control: a 68% decrease in BV/TV at 0.1 kHz ($P < 0.01$) and 36% decrease in BV/TV at 1 kHz ($P < 0.05$) (Figure 1e).

3.2. Treatment of the Matrigel with DBD alters chondrogenesis and cell proliferation/migration

Histological staining of the Matrigel masses with Alcian Blue highlighted the cartilage-rich regions of each treatment (Figure 2a). A more careful examination of the Alcian Blue-stained regions was performed to determine how treatment of the Matrigel with DBD had affected chondrogenesis. Quantification of the Alcian Blue-stained area per total area showed significant increases in the per cent cartilage area after 0.1 kHz nsp DBD and 1 kHz

nsp DBD, respectively, compared with control ($P < 0.05$) (Figure 2b). No significant difference was observed for μsp DBD. To study the effect of DBD treatment on cell number, DAPI fluorescent labelling was used to visualize cell nuclei (Figure 2c). Quantitative analysis of the area of DAPI staining per total area revealed that masses where the Matrigel was treated with μsp DBD had an increase in DAPI fluorescent area. The nsp DBD treatment of the Matrigel at 1 kHz showed no change from control, while nsp DBD treatment of the Matrigel at 0.1 kHz showed a decrease in DAPI-stained area (Figure 2d). These findings indicate the μsp DBD-treated masses contained a greater percentage of cells compared with controls, indicating enhanced cell proliferation or migration into the Matrigel, or a combination of both.

3.3. DBD alters the ECM to influence chondrocyte physiology and morphology

Vascular invasion is required for bone to form as the result of endochondral ossification. To determine if this process was affected by the DBD treatment of Matrigel immunohistochemical staining was performed to show cartilage expression of VEGF. Qualitative differences in the distribution and pattern of VEGF staining were observed between all treatments (Figure 3a, ×10 magnification). The expression of VEGF stained area normalized by total area was measured by automated image analysis. When compared with untreated control, the μsp DBD-treated Matrigel showed a significant increase in VEGF staining of the Matrigel mass ($P < 0.001$); in contrast, the nsp DBD-treated Matrigel from both frequencies had significantly decreased VEGF expression ($P < 0.001$) (Figure 3b).

3.4. Fibroblast proliferation induced response to DBD-treated Matrigel

After injection, the Matrigel creates a mild inflammatory response within the host, which causes mesenchymal cell migration into the Matrigel. To determine if differences in the inflammatory response between the DBD-treated Matrigel was present the thickness of the fibrotic ring of cells surrounding each mass (indicating fibroblast proliferation) were measured. Formation of a layer of fibroblastic cells is a common foreign body response of the host cells indicating an inflammatory response. Images of the perimeter of the haematoxylin and eosin (H&E)- and Alcian Blue-stained Matrigel mass from each treatment group show a thicker band of fibroblast cells around the nsp DBD- treated masses (Figure 3c, white brackets). Automated image analysis quantifying the area of the fibroblasts around the mass normalized by the total area of the mass revealed that significantly more fibroblasts had surrounded the nsp DBD-treated Matrigel, while μsp DBD-treated Matrigel showed no differences from control (Figure 3d).

3.5. DBD modifies type IV collagen within the Matrigel

Masson's trichrome, a histological stain for collagen (blue), was used to stain the cell-free areas of Matrigel not occupied by cartilage or bone (Figure 4a, high magnification images). The cell-free areas of Matrigel stained blue, owing to the presence of type IV collagen, in both control and μsp DBD-treated masses. Interestingly, in both of the nsp DBD-treated samples the cell-free collagen-rich regions stained bright red. To determine if the collagen had been cleaved or altered, all three samples were analysed by SDS-PAGE and FT-IRIS, Electrophoretic analysis of Matrigel showed no alterations in banding patterns of any treatment compared with untreated Matrigel, indicating no cleavage of ECM components in

the Matrigel (Figure 4b). The second derivative FT-IRIS spectra for pure type IV collagen, untreated Matrigel (Control) and Matrigel treated with μsp DBD and nsp DBD were very similar (Figure 4c). However, type IV collagen exhibited an amide I absorbance at 1624/cm, which was not present in control and treated Matrigel samples. All the DBD-treated Matrigel samples showed broadening of the amide I region centred at ~1650/cm, and an additional peak absorbance at 1671/cm associated with turn structures in proteins (Barth, 2007) (Figure 4c).

3.6. DBD-treated collagen modifies cell protein expression

Because Matrigel is a complex mixture of ECM molecules where collagen is only one component among other proteins and growth factors, a simpler model was necessary to determine how DBD modification of collagen affected cell signalling/behaviour. To investigate this, type I collagen from rat tail was treated using the same methods as previously used to treat the Matrigel. Changes in the expression of focal adhesion kinase (pFAK and FAK), protein kinase B (Akt), B-cell lymphoma 2 (Bcl-2) and cytochrome C (CytC) were analysed using western analysis. Cells cultured in flasks that were coated with μsp DBD-treated collagen showed increased expression of all proteins, except CytC, which was not present. Cells cultured with nsp DBD-treated collagen showed a decrease in the expression of all proteins, and the decrease appeared to be dose dependent, with a greater decrease in the 1 kHz treatment compared with the 0.1 kHz treatment (Figure 5a). In addition, both nsp DBD treatments induced the expression of CytC, an indicator of mitochondrial stress. Protein expression of cells cultured in control flasks lacking collagen did not differ from cells cultured with untreated collagen, indicating that collagen coating of culture flasks does not alter protein expression. Further, fluorescent images of cells stained with phalloidin (actin) and DAPI showed decreased spreading in cultures on cover slips coated with nsp DBD-treated collagen (Figure 5b), compared with control or μsp DBD-treated collagen. Finally, to test whether μsp DBD was capable of eliciting a similar response, the highest frequency setting available on the μsp DBD device (3.5 kHz, same voltage) was used to treat the collagen. At this setting, similar decreases in the expression of the four proteins were observed along with cell morphology changes similar to those of cells grown on the nsp DBD-treated collagen (see the Supplementary material online, Figure S1).

3.7. Nanosecond DBD generates increased ROS and RNS

To investigate whether differences in ROS and RNS generation by μsp DBD and nsp DBD might address differences observed in the reactions with the ECM, the amount of H_2O_2, nitric oxide (NO) and peroxynitrite anion ($ONOO^-$) generated by plasma was measured. A 10% gelatin solution was used as a substitute for Matrigel and H_2O_2, NO and $ONOO^-$ concentrations were determined in a solid gelatin after it was treated (Figure 6a–c). The H_2O_2 production was increased with DBD treatment time for all DBD plasma conditions. However, the H_2O_2 production by μsp-DBD was significantly lower (approximately 1/2 to 1/3) than either nsp DBD treatments (Figure 4a; $P < 0.05$) at 30, 60 and 120 s. In addition, nsp at 0.1 kHz was significantly lower ($P < 0.05$) than at 1 kHz at 60 s and 120 s.

Similarly, RNS production in response to both nsp DBD treatments resulted in higher NO and $ONOO^-$ production (1.5–2 times) compared with μsp DBD at every time-point (Figure

4b,c; $P < 0.05$). After 1 min of treatment, the intensity of fluorescence showed no further increase in NO concentration in response to any of the three treatments (Figure 4b). In contrast, only the μsp DBD treatment showed saturation of $ONOO^-$ after 1 min (~30 a.u.). Further, unlike the NO or H_2O_2 production, the highest $ONOO^-$ production was observed for the 0.1 kHz nsp DBD treatment rather than the 1 kHz nsp DBD treatment (Figure 6c; $P < 0.05$ for μsp DBD vs. nsp DBD at 0.1 kHz and $P < 0.05$ for nsp DBD at 0.1 kHz compared with 1 kHz).

4. Discussion

The present study evaluated the effect of μsp DBD or nsp DBD modification of Matrigel ECM on the host cell response in the murine ectopic ossification model. Pretreatment of Matrigel with μsp DBD enhanced cell infiltration/numbers, VEGF production, chondrocyte differentiation and increased bone formation. These effects were significantly lower after nsp DBD treatment at either a comparable power (nsp DBD treatment at pulse repetition rate of 0.1 kHz, 0.8 W) or pulse repetition rate (1 kHz, 9.7 W) to μsp DBD treatment (1 kHz, 1.1 W). The main treatment differences included the increased production by nsp DBD of H_2O_2, NO and $ONOO^-$, the extent of Matrigel collagen modification and the decrease in FAK activation. These results demonstrate that plasma changes to the Matrigel ECM could effectively enhance or inhibit ECM–cell interactions to alter cellular function and endochondral bone formation. Thus, depending on the DBD plasma treatment, the ECM can be differentially modified to either enhance or disrupt ECM–cell interactions as required for a specific clinical and/or tissue engineering application.

Although the present study controlled for power or frequency to compare μsp DBD with nsp DBD, it is challenging to directly compare these discharges as multiple differences exist. It was reported that nsp DBD discharges are less filamentary and more uniform than those of μsp DBD (Ayan *et al.*, 2008). Additional physical differences include the magnitude of the local electric field, thermal differences, the filament-initiated shock wave and the emitted radiation (Fridman *et al.*, 2008). Each of these factors has the ability to directly modify ECM (Bassett *et al.*, 1982; Brighton *et al.*, 1985; Goodship and Kenwright, 1985; Kenwright and Goodship, 1989; Pilla *et al.*, 1990; Joyce *et al.*, 1990; Heckman, 1994; Fredericks *et al.*, 2000) and therefore are predicted to have different biological outcomes. With the increasing number of plasma medicine applications, it is imperative to acquire a better understanding of μsp DBD and nsp DBD effects on both ECM and cellular activity. Accordingly, the present study selected conditions that evaluated μsp DBD and nsp DBD at either comparable power (0.8–1.1 W) or frequency (1 kHz) in an effort to define biological differences and outcomes.

After nsp DBD treatment, a difference in collagen (ECM) staining was observed in the Matrigel using trichrome histology. In the staining protocol, an acidic red dye is used that binds all basic tissue components; a weak acid wash then removes the red dye from the less basic collagen component and an acidic blue dye selectively binds the collagen. Instead of staining blue, the collagen appeared red, indicating that nsp DBD changed the basic nature of the collagen. A plausible explanation is that the higher production of H_2O_2, NO and $ONOO^-$ by nsp DBD modified the amino acid side-chains and thus altered the basic nature of collagen. Specifically, the RNS, $ONOO^-$, is known to react with proline/hydroxyproline

(prevalent in collagen) and produce the more basic *N*-nitrosopyrrolidine amino acid, by converting the carbonyl to a nitroso group (Ahmad and Ahsan, 2011). Supporting a change in amino acid chemistry, as opposed to a structural change or cleavage, analysis of both Matrigel and type IV collagen by FTIR and western blot showed no detectable differences between μsp DBD and nsp DBD treatment. Together, these results suggest the modification of the amino acid side-chains may be responsible for the decreased bone formation after nsp DBD treatment.

While it is possible that the lower production of $ONOO^-$ by μsp DBD may modify the amino acid side-chains to increase bone formation, previous studies have shown that biophysical stimuli such as electric fields, ultrasound and mechanical strain can enhance endochondral ossification during fracture repair by altering cell interactions with the ECM (Bassett *et al.*, 1982; Brighton *et al.*, 1985; Goodship and Kenwright, 1985; Kenwright and Goodship, 1989; Pilla *et al.*, 1990; Joyce *et al.*, 1990; Heckman, 1994; Fredericks *et al.*, 2000). Other studies that specifically investigated the direct effects of biophysical stimuli and reactive species on ECM found that structural or conformational alterations exposed 'matricryptic' sites on ECM proteins and carbohydrate groups (Davis *et al.*, 2000). These sites are commonly exposed at sites of tissue injury and enhance cell–ECM interactions (Davis *et al.*, 2000), leading to the activation of signalling pathways that facilitate tissue repair (Reing *et al.*,). In addition, biophysical stimuli and injury generate biologically active ECM peptide fragments, termed 'matricryptins,' (Beattie *et al.*, 2008; Reing *et al.*, 2008; Tottey *et al.*, 2011). Matricryptins enhance cell migration to the local area and cell proliferation, creating favourable conditions for tissue remodelling.

The complexity of Matrigel, a mixture of collagen IV, laminin, entactin, cytokines, hormones and growth factors, makes it impossible to determine the plasma modifications to each component (Hughes *et al.*, 2010). Thus, in an effort to understand the μsp DBD- and nsp DBD-specific effects on a single ECM component, isolated rat tail type I collagen was subjected to the same DBD treatments used on the Matrigel. Analysis of protein expression by mesenchymal cells grown on the treated collagen showed that μsp DBD treatment increased pFAK, FAK and the total cell number compared with nsp DBD treatment. Increases in pFAK and FAK indicate enhanced adhesion or cell–ECM interaction through integrin binding (Zachary, 1997). In addition, pFAK enhances chondrogenic differentiation, which may account for the increases in hypertrophic chondrocytes, VEGF and bone formation observed in Matrigel treated with μsp DBD. Furthermore, increases in the anti-apoptotic proteins Akt and Bcl-2 suggest that the cells grown on μsp DBD-treated collagen are less susceptible to apoptosis and cell death. All of these changes support the possibility that increases in both the number of cells entering chondrogenesis and the rate of chondrogenic differentiation are enhanced in response to the μsp DBD-treated Matrigel/ECM, resulting in increased bone formation. Notably, when μsp DBD is used at the highest setting (3.5 kHz) the expression of pFAK, FAK, Akt and Bcl-2 were decreased compared with the untreated collagen, indicating the positive or negative cell–ECM interaction is not specifically determined by the DBD pulse rate (see Figure S1, Supplementary material online).

The results of the present study show that ECM molecules can be differentially modified by DBD treatment to positively or negatively affect bone formation. The greater amounts of ROS and RNS generated by DBD treatment correlated with the modification of collagen and a negative effect on chondrogenic differentiation and bone formation. The present work highlights the importance of tailoring DBD treatment for each plasma medicine or tissue engineering application and provides insight into the potential differences in the biological outcomes that result when using μsp DBD vs. nsp DBD.

Supplementary Material

Refer to Web version on PubMed Central for supplementary material.

Acknowledgments

The authors thank Carol Diallo, Deepa Kurpad and Dr Qian-Shi Zhang for their help with the project and μCT analysis. Special thanks go to Drs Gary Friedman, Greg Fridman and Alex Fridman for their valuable discussions. This work was supported by NIH Grant R01 EB 013011-01 (T.F.).

References

Ahmad, R., Ahsan, H. Autoimmune Disorders – Pathogenetic Aspects. Mavragani CP. InTech; Rijeka, Croatia: 2011. Contribution of Peroxynitrite, a Reactive Nitrogen Species, in the Pathogenesis of Autoimmunity; p. 141-156.

Alekseev O, Donovan K, Limonnik V, et al. Nonthermal dielectric barrier discharge (DBD) Plasma suppresses Herpes Simplex Virus Type 1 (HSV-1) replication in corneal epithelium. Transl Vis Sci Technol. 2014; 3:2.

Ayan H, Fridman G, Gutsol AF, et al. Nanosecond-pulsed uniform dielectric-barrier discharge. Plasma Sci IEEE Trans. 2008; 36:504–508.

Barth A. Infrared spectroscopy of proteins. Biochim Biophys Acta. 2007; 1767:1073–1101. [PubMed: 17692815]

Bassett C, Valdes MG, Hernandez E. Modification of fracture repair with selected pulsing electromagnetic fields. J Bone Joint Surg Am. 1982; 64:888–895. [PubMed: 7085716]

Beattie AJ, Gilbert TW, Guyot JP, et al. Chemoattraction of progenitor cells by remodeling extracellular matrix scaffolds. Tissue Eng Part A. 2008; 15:1119–1125.

Brighton CT, Hozack WJ, Brager MD, et al. Fracture healing in the rabbit fibula when subjected to various capacitively coupled electrical fields. J Orthop Res. 1985; 3:331–340. [PubMed: 2411896]

Brulle L, Vandamme M, Ries D, et al. Effects of a non thermal plasma treatment alone or in combination with gemcitabine in a MIA PaCa2-luc orthotopic pancreatic carcinoma model. PLoS One. 2012; 7:e52653. [PubMed: 23300736]

Chernets N, Zhang J, Steinbeck M, et al. Non-thermal atmospheric pressure plasma enhances mouse limb bud survival, growth and elongation. Tissue Eng. 2014; 21:300–309.

Chernets N, Kurpad DS, Alexeev V, et al. Reaction chemistry generated by nanosecond pulsed dielectric barrier discharge treatment is responsible for the tumor eradication in the B16 melanoma mouse model. Plasma Process Polym. 2015; 12:1400–1409. [PubMed: 29104522]

Daeschlein G, Napp M, Lutze S, et al. Skin and wound decontamination of multidrug-resistant bacteria by cold atmospheric plasma coagulation. J Dtsch Dermatol Ges. 2015; 13:143–150. [PubMed: 25597338]

Davis GE, Bayless KJ, Davis MJ, et al. Regulation of tissue injury responses by the exposure of matricryptic sites within extracellular matrix molecules. Am J Pathol. 2000; 156:1489–1498. [PubMed: 10793060]

Dobrynin D, Fridman G, Friedman G, et al. Deep penetration into tissues of reactive oxygen species generated in floating-electrode dielectric barrier discharge (FE-DBD): an *in vitro* agarose gel model mimicking an open wound. 2012; 2:71–83.

Duval A, Marinov I, Bousquet G, et al. Cell death induced on cell cultures and nude mouse skin by non-thermal, nanosecond-pulsed generated plasma. PLoS One. 2013; 8:e83001. [PubMed: 24358244]

Eaton GJ, Zhang QS, Diallo C, et al. Inhibition of apoptosis signal-regulating kinase 1 enhances endochondral bone formation by increasing chondrocyte survival. Cell Death Dis. 2014; 5:e1522. [PubMed: 25393478]

Fredericks DC, Nepola JV, Baker JT, et al. Effects of pulsed electromagnetic fields on bone healing in a rabbit tibial osteotomy model. J Orthop Trauma. 2000; 14:93–100. [PubMed: 10716379]

Fridman, A. Plasma Chemistry. Cambridge University Press; Cambridge: 2008.

Fridman G, Peddinghaus M, Balasubramanian M, et al. Blood coagulation and living tissue sterilization by floating-electrode dielectric barrier discharge in air. Plasma Chem Plasma Process. 2006; 26:425–442.

Fridman G, Friedman G, Gutsol A, et al. Applied plasma medicine. Plasma Process Polym. 2008; 5:503–533.

Goodship A, Kenwright J. The influence of induced micromovement upon the healing of experimental tibial fractures. J Bone Joint Surg. 1985; 67:650–655. [PubMed: 3980515]

Heckman J. Acceleration of tibial fracture healing by non-invasive, low-intensity pulsed ultrasound. J Bone Joint Surg. 1994; 76:26–34. [PubMed: 8288661]

Hughes CS, Postovit LM, Lajoie GA. Matrigel: a complex protein mixture required for optimal growth of cell culture. Proteomics. 2010; 10:1886–1890. [PubMed: 20162561]

Jiang C, Chen MT, Gorur A, et al. Nanosecond pulsed plasma dental probe. Plasma Process Polym. 2009; 6:479–483.

Joyce ME, Terek RM, Jingushi S, et al. Role of transforming growth factor-beta in fracture repair. Ann N Y Acad Sci. 1990; 593:107–123. [PubMed: 2197959]

Kenwright J, Goodship AE. Controlled mechanical stimulation in the treatment of tibial fractures. Clin Orthop Relat Res. 1989; 241:36–47.

Kong MG, Kroesen G, Morfill G, et al. Plasma medicine: an introductory review. N J Phys. 2009; 11:115012.

Li Y, Kojtari A, Friedman G, et al. Decomposition of l-valine under nonthermal dielectric barrier discharge plasma. J Phys Chem B. 2014; 118:1612–1620. [PubMed: 24450953]

Li Y, Sun K, Ye G, et al. Evaluation of cold plasma treatment and safety in disinfecting 3-week root canal *Enterococcus faecalis* biofilm *in vitro*. J Endod. 2015; 41:1325–1330. [PubMed: 26027875]

Liu C, Dobrynin D, Fridman A. Uniform and non-uniform modes of nanosecond-pulsed dielectric barrier discharge in atmospheric air: fast imaging and spectroscopic measurements of electric field. J Phys D Appl Phys. 2014; 47:252003. [PubMed: 25071294]

Park D, Fridman G, Fridman A, et al. Plasma bullets propagation inside of agarose tissue model. Plasma Sci IEEE Trans. 2013; 41:1725–1730.

Pilla A, Mont M, Nasser P, et al. Non-invasive low-intensity pulsed ultrasound accelerates bone healing in the rabbit. J Orthop Trauma. 1990; 4:246–253. [PubMed: 2231120]

Reing JE, Zhang L, Myers-Irvin J, et al. Degradation products of extracellular matrix affect cell migration and proliferation. Tissue Eng Part A. 2008; 15:605–614.

Siu A, Volotskova O, Cheng X, et al. Differential effects of cold atmospheric plasma in the treatment of malignant glioma. PLoS One. 2015; 10:e0126313. [PubMed: 26083405]

Steinbeck MJ, Chernets N, Zhang J, et al. Skeletal cell differentiation is enhanced by atmospheric dielectric barrier discharge plasma treatment. PLoS One. 2013; 8:e82143. [PubMed: 24349203]

Tottey S, Corselli M, Jeffries EM, et al. Extracellular matrix degradation products and low-oxygen conditions enhance the regenerative potential of perivascular stem cells. Tissue Eng Part A. 2011; 17:37–44. [PubMed: 20653348]

Ulrich C, Kluschke F, Patzelt A, et al. Clinical use of cold atmospheric pressure argon plasma in chronic leg ulcers: a pilot study. J Wound Care. 2015; 24:196, 198–200, 202–193. [PubMed: 25970756]

Zachary I. Focal adhesion kinase. Int J Biochem Cell Biol. 1997; 29:929–934. [PubMed: 9375372]

Zhang S, Jia L, Wang W-C, et al. The influencing factors of nanosecond pulse homogeneous dielectric barrier discharge in air. Spectrochim Acta Part A. 2014; 117:535–540.

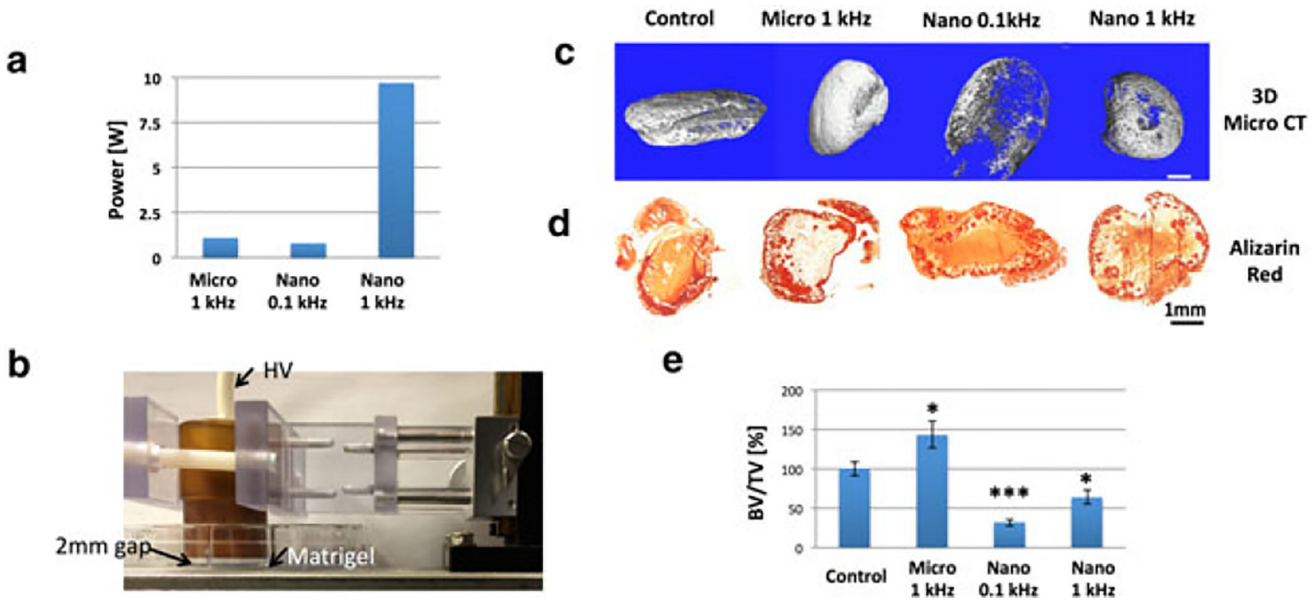

Figure 1.

Dielectric barrier discharge (DBD) treatment of Matrigel effects bone formation. (a) Plasma power measurement comparing 1 kHz microsecond pulsed (μsp) DBD treatment (1.1 W), 0.1 kHz nanosecond pulsed (nsp) DBD treatment (0.8 W) and 1 kHz nsp DBD (9.7 W). (b) Apparatus for DBD plasma treatment included an insulated copper electrode with a high voltage (HV) connection to the power source (either μs or ns pulser) positioned 2 mm from the ice-cooled liquid Matrigel in a six-well plate. (c) Three-dimensional image analysis by microcomputed tomography showed visual representation of bone formation in the masses. (d) Alizarin Red staining of cross-section of each mass allowed for visualization of calcium deposits (red-stained regions of bone formation). (e) Microcomputed tomography analysis of bone volume per total volume (BV/TV) represents quantitative analysis of bone formation. Treatment with 1 kHz μsp DBD resulted in a 43% increase in BV/TV ($P < 0.05$), while 0.1 kHz nsp DBD treatment resulted in a 68% decrease in BV/TV ($P < 0.01$) and 1 kHz nsp DBD treatment resulted in a 36% decrease in BV/TV ($P < 0.05$). $n = 8$ for 1 kHz μsp DBD and nsp DBD; $n = 4$ for 0.1 kHz nsp DBD. *$P < 0.05$, ***$P < 0.001$. Bar: 1 mm.

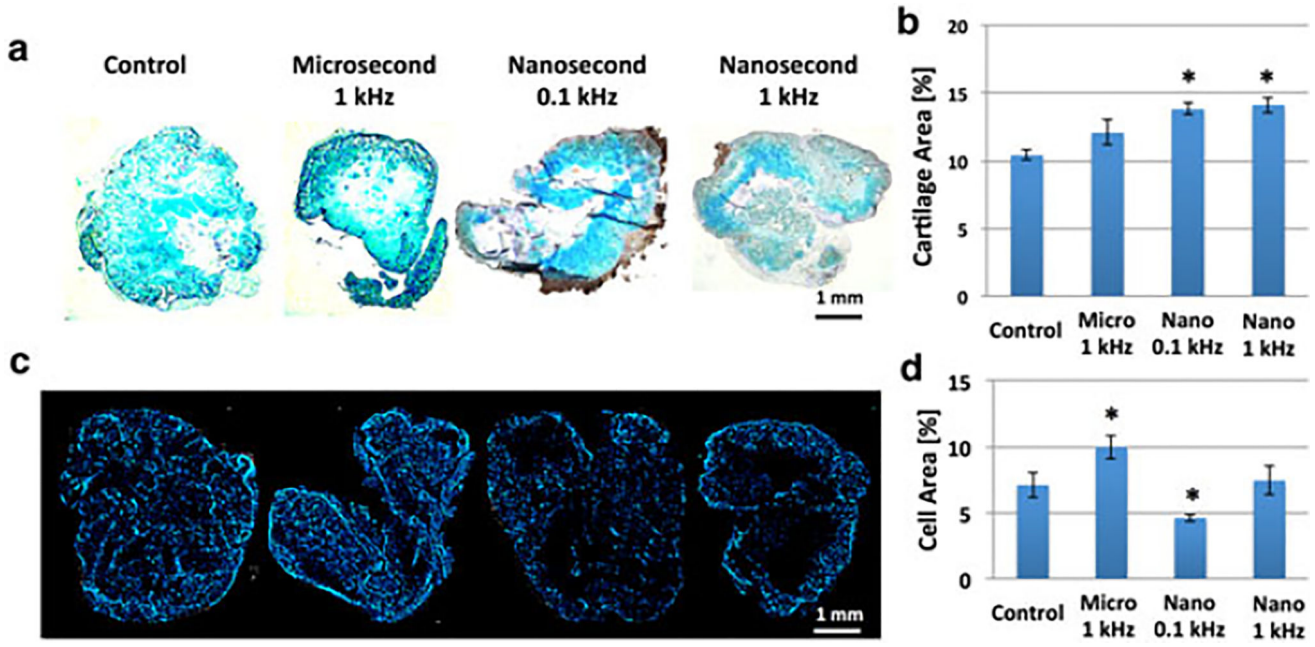

Figure 2.

Dielectric barrier discharge (DBD) treatment of Matrigel alters chondrogenesis, cell migration and proliferation. (a) Alcian Blue staining allowed for specific analysis of cartilage-rich regions in sections of masses. (b) Quantitative analysis of stained regions via ImagePro Plus software showed an increase in per cent cartilage area in 0.1 kHz and 1 kHz nanosecond pulsed (nsp) DBD, respectively ($P < 0.05$). These results indicate that there are greater cartilage-rich regions present in masses treated with nsp DBD. (c) Fluorescent analysis with 4′,6-diamidino-2-phenylindole (DAPI) allowed for visualization of cell migration and proliferation in sections of masses. (d) Quantitative analysis of DAPI stain via ImagePro Plus software showed an increase in the per cent cell area in masses treated with 1 kHz microsecond pulsed (μsp) DBD ($P < 0.05$). Masses treated with 0.1 kHz nsp DBD showed a decrease in per cent cell area ($P < 0.05$). $n = 4$ for all treatments in Alcian Blue analysis. $n = 6$ for DAPI analysis for 1 kHz μsp DBD and nsp DBD, and $n = 4$ for 0.1 Hz nsp DBD. *$P < 0.05$. Bar: 1 mm.

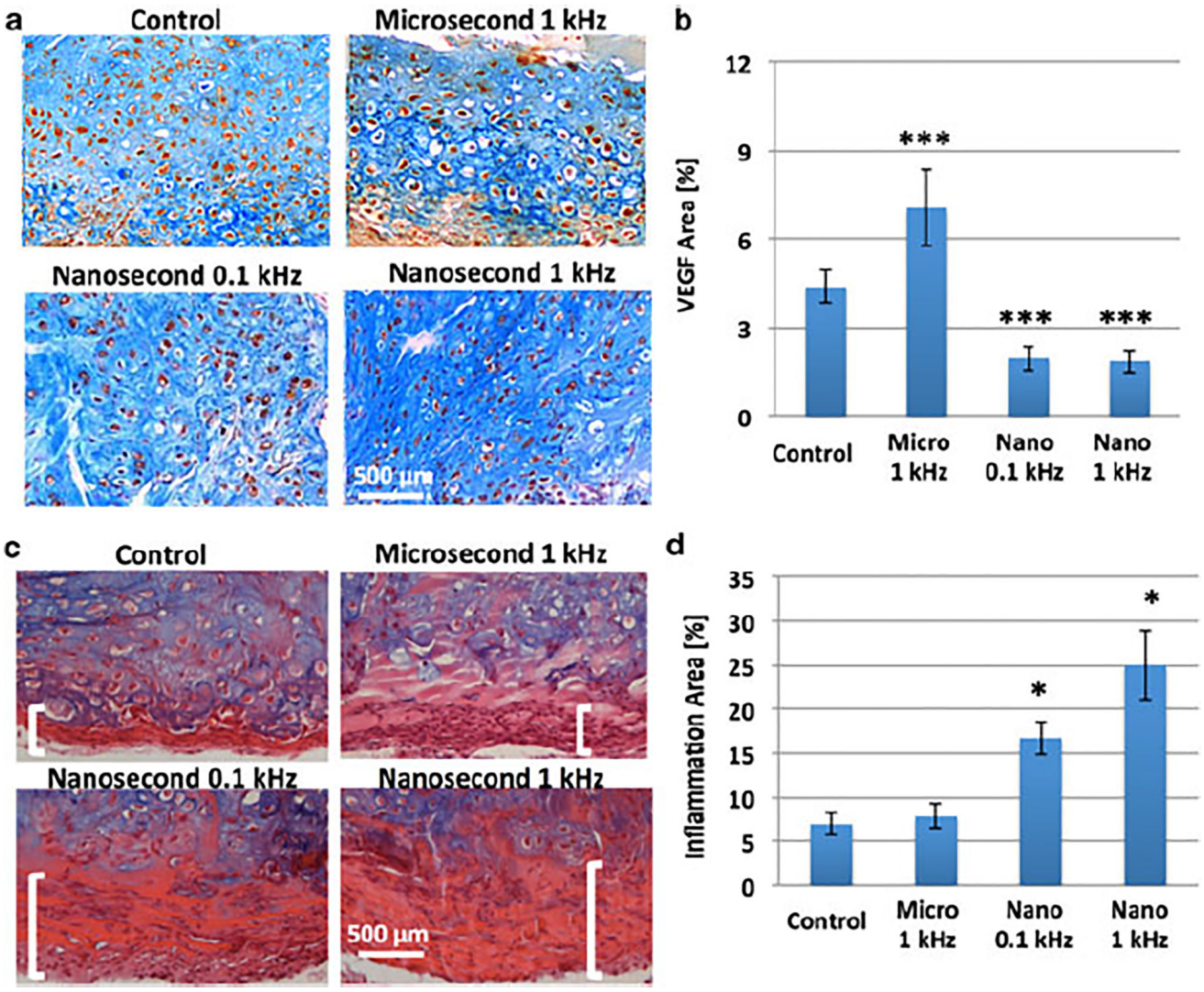

Figure 3.

Dielectric barrier discharge (DBD) treatment effects on chondrocyte physiology and morphology. (a) Immunohistochemical staining showed vascular endothelial growth factor (VEGF) production (brown staining) and chondrocyte hypertrophy (cells with white spaces) was increased with microsecond pulsed (µsp) DBD treatment. (b) Quantitative analysis of VEGF confirmed increased VEGF in 1 kHz microsecond pulsed (µsp) DBD-treated masses, while nsp-DBD treatment at 0.1 kHz and 1 kHz had decreased VEGF compared with control. (c) Haematoxylin and eosin/Alcian Blue stain highlights thickened (red) regions of collagen production by fibroblast on the perimeter of Matrigel mass (white brackets) representing the foreign body inflammatory response. (d) Quantitative analysis showed an increase in inflammatory fibrotic ring surrounding the masses treated with nsp DBD at 0.1 kHz and 1 kHz, respectively. $n = 4$; $*P < 0.05$, $***P < 0.001$. Bar: 500 µm.

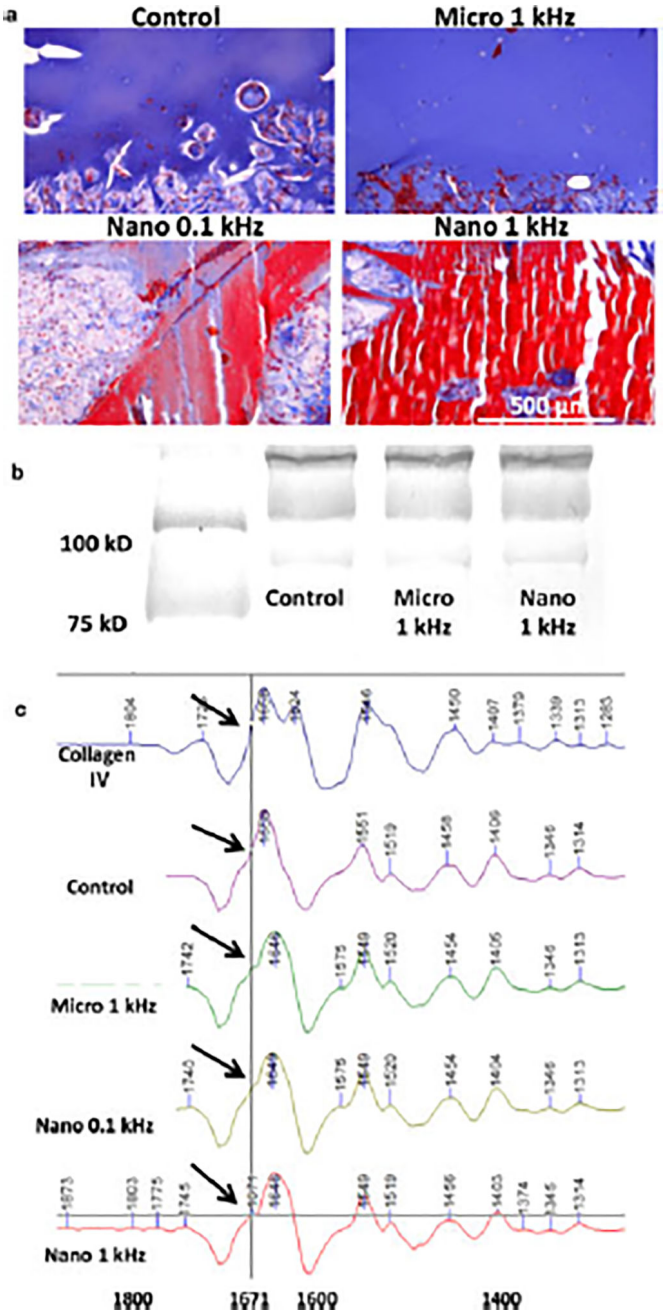

Figure 4.

Modification of collagen by dielectric barrier discharge (DBD) treatment. (A) Trichrome staining shows the collagen from the nanosecond pulsed (nsp) DBD-treated Matrigel stains; red staining indicates an alteration of collagen compared with the normal blue staining of collagen in control and microsecond pulsed (µsp) DBD-treated Matrigel. (b) Sodium dodecyl sulphate–polyacrylamide gel electrophoresis performed on control, 1 kHz µsp DBD- and 1 kHz nsp DBD-treated Matrigel samples gave in similar band patterns, indicating that none of the DBD treatments alter Matrigel by proteolysis. (c) Fourier transform infrared imaging spectroscopy analysis of Matrigel samples; second derivative

analysis shows the broadening of the amide I contour centred at ~1650/cm and the addition of a peak absorbance at 1671/cm (black arrows) in DBD-treated samples, associated with protein turn structures. Bar: 500 μm.

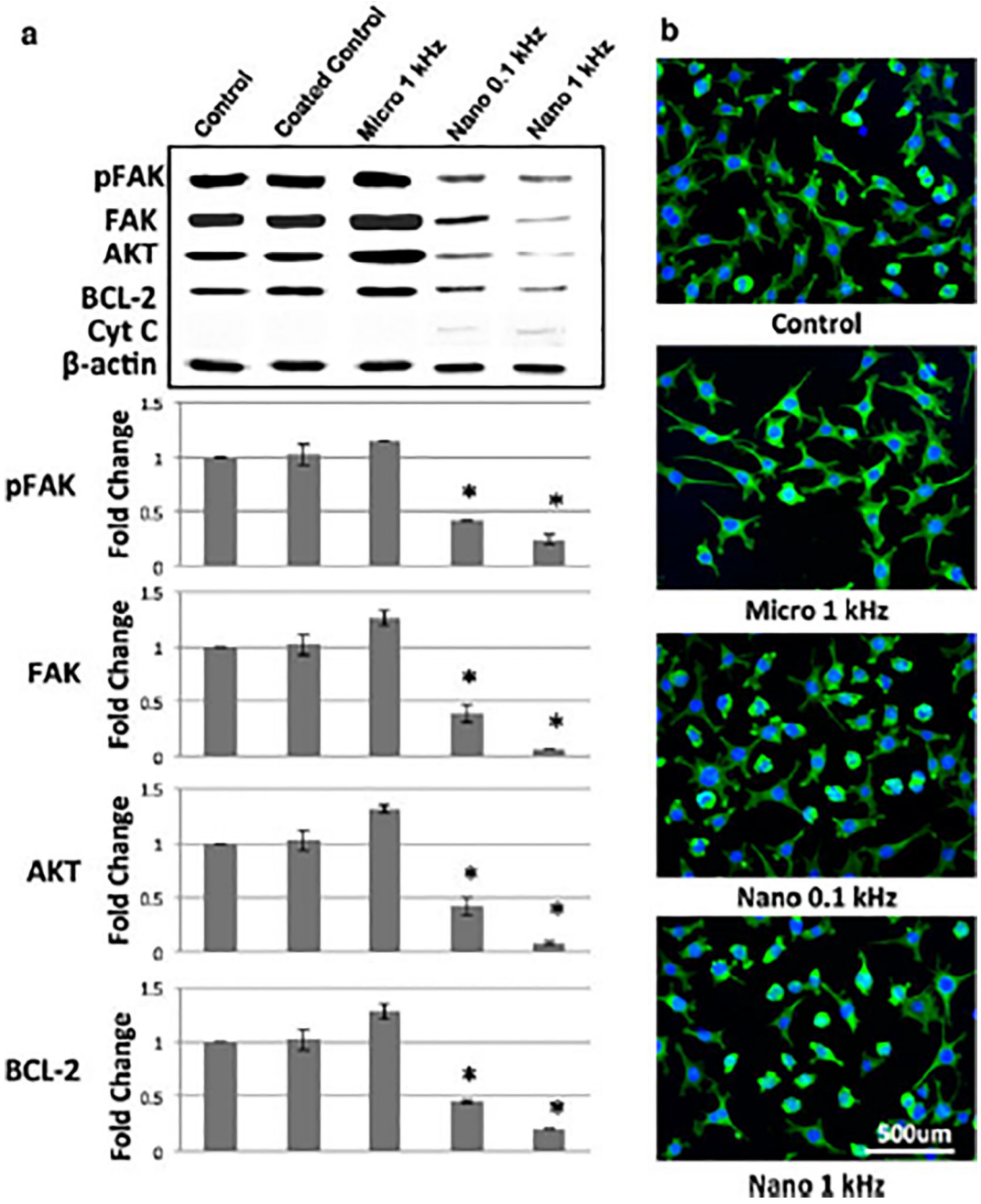

Figure 5.

Dielectric barrier discharge (DBD) treatment of type I collagen modifies cell protein expression. (a) The 24-h culture of C3H/10 T1/2 cells cultured with DBD-treated collagen shows altered levels of phosphorylated focal adhesion kinase (pFAK), focal adhesion kinase (FAK), protein kinase B (Akt) and B-cell lymphoma 2 (Bcl-2), compared with control. Culture with type I collagen treated with microsecond pulsed (μsp) DBD 1 kHz plasma increased each protein amount when compared with control. Collagen treated with both nanosecond pulsed (nsp) DBD at 0.1 kHz and 1 kHz both resulted in decreased protein levels; however 1 kHz nsp DBD treatment showed a greater decrease. Both nsp DBD

treatments showed increases in cytochrome C (CytC), while control and μsp DBD treatments did not. Untreated type I collagen coated onto cell culture flasks (Coated Control) did not induce changes relative to uncoated control flasks. All proteins are normalized to actin and represented as up- or down-regulation relative to control. (b) Fluorescent imaging of DBD-treated cells after 6 h of culture. Blue indicates 4′,6-diamidino-2-phenylindole (DAPI) stain, green indicates actin. Bar: 500 μm.

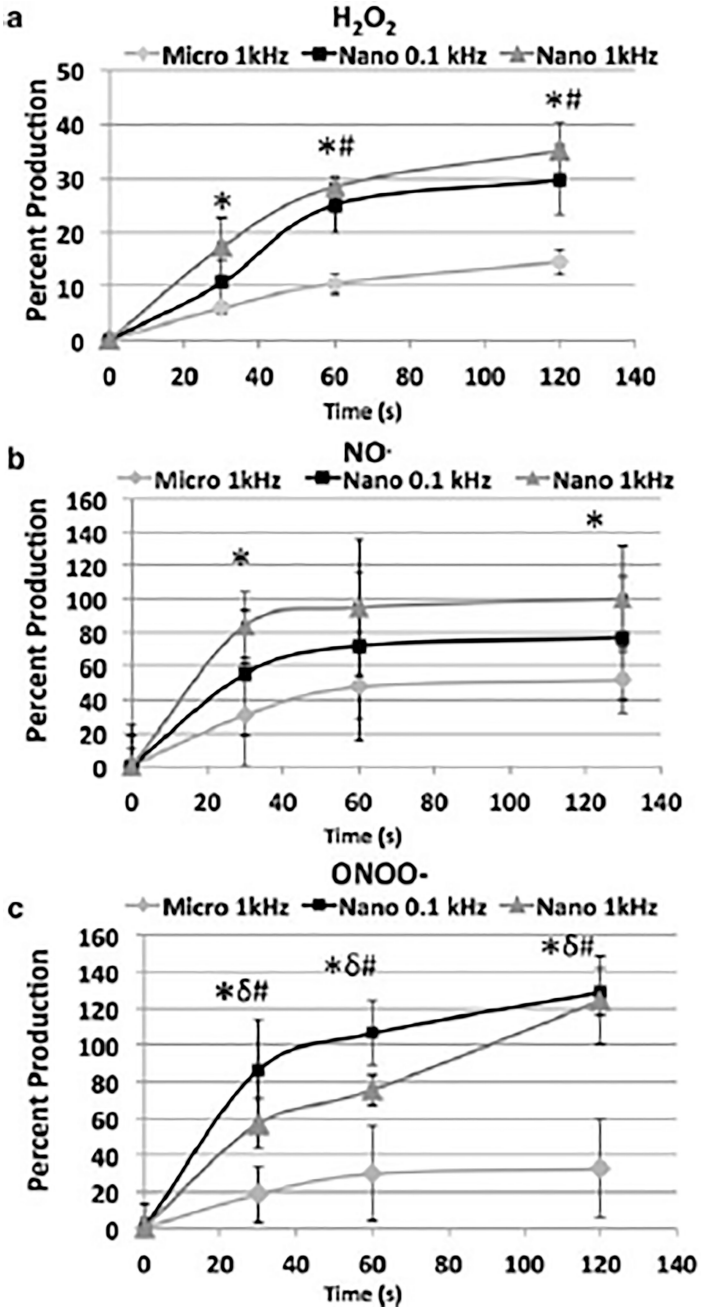

Figure 6.

Dielectric barrier discharge (DBD) treatment produces reactive species in gelatin. (A) Hydrogen peroxide (H_2O_2) production in solidified gelatin (10% gelatin) was measured using Amplex UltraRed reagent for H_2O_2 concentration as a function of time. Nanosecond pulsed (nsp) DBD treatments produce 2.5–2.7 times higher amounts of H_2O_2 compared with microsecond pulsed (μsp) DBD treatment at 60 s of treatment. (b) Nitric oxide (NO) production in solidified gelatin (10% gelatin) was measured with diaminofluorescein-2 (DAF-2) reagent for NO concentration over time. The nsp-DBD treatment produces 1.5–2 times greater concentration of NO compared with μsp DBD treatment. (c) Peroxynitrite

(ONOO⁻) production in solidified gelatin (10% gelatin) was measured with dichlorodihydrofluorescein diacetate (H_2DCFDA) reagent for ONOO⁻ concentration as a function of time. The nsp DBD treatment produces 3–4 times greater concentration of ONOO⁻ compared with the μsp DBD treatment. *, $P < 0.05$, comparing μsp DBD with nsp DBD at 1 kHz; δ, $P < 0.05$; comparing 1 kHz μsp DBD with 0.1 kHz nsp DBD; #, $P < 0.05$, comparing 0.1 kHz nsp DBD with 1 kHz nsp DBD.